Direction of Arrival Estimation Apparatus for Communication Based Train Control System using ESPAR Antenna

Julian Webber, Satoshi Tsukamoto, Susumu Ano, Naoya Kukutsu and Tomoaki Kumagai
Advanced Telecommunications Research Institute International, 2-2-2, Hikaridai, Seika-cho, Kyoto, 619-0288, Japan
{**jwebber, tsukamoto, ano, kukutsu, kumagai**}**@atr.jp**

***Abstract*—A 12-element Electronically Steerable Parasitic Array Radiator (ESPAR) antenna system has been designed for direction-of-arrival (DoA) estimation as part of a railway control system. The DoA is estimated using the cross-correlation and MUSIC algorithms. Whilst a majority of reported DoA estimation systems typically operate in wideband WLAN or ISM band systems with a static condition, our narrowband system operates with mobility in the UHF band at 4800 Baud within about a 6.5 kHz bandwidth. Our experimental results show that the developed system can estimate the number of the component multi-path waves.**

***Keywords*—**ESPAR antenna, direction-of-arrival, cross-correlation, MUSIC, beam-forming, train radio system.

I. Introduction

Improved communication and connectivity of digital train radio is essential for the reliability of a communication-based train control system. In order to decide the positions of base station antennas and their direction, an antenna based direction of arrival (DoA) estimation system is desired. Although the system uses a directional antenna for reducing inevitable multi-path fading, the DoA of the component multi-path waves should be estimated. However, at the UHF frequencies employed for digital train radio, a Yagi-Uda antenna would be excessively large, particularly in the confined space of the train roof or working-train deck. A traditional circular array beam forming system employing an array of active antenna elements is also cumbersome. Therefore, we have designed an Electronically Steerable Parasitic Array Radiator (ESPAR) antenna system for DoA estimation.

An ESPAR antenna has a single active RF port which considerably reduces the cost and size of circuitry. The antenna has gained considerable popularity since a practical implementation of beam steering by a single active radiator surrounded by passive radiators was first demonstrated around year 2000 [1]. By controlling the switching of the passive elements, called parasitic elements, it is possible to scan the main beam to any 360 degree direction. ESPAR antennas have received much interest as part of distributed remote radio head (RRH) systems due to their low-cost, compact size and low-power requirements e.g. [2].

In this work, the signal DoA is estimated using the cross-correlation and high-resolution MUSIC (MUltiple SIgnal Classification) algorithms. In contrast to the majority of MUSIC algorithms typically being applied to the wide band system, such as wireless local area network system with static condition in the ISM or 5 GHz bands here we operate a narrow band system, with mobility in UHF band. ISM band has a 20 MHz channel separation and the band width of 802.11 is about 16 MHz depending on the modulation i.e. OFDM or DSSS etc. The UHF standard defines a 5.8 kHz band width and 6.25 kHz channel separation.

The layout of this paper is as follows. The ESPAR antenna is described in Section II and details of the DoA estimation algorithms are outlined in Section III. The experimental system is described in Section IV with performance results discussed in Section V. Further work is outlined in Section VI and a conclusion drawn in Section VII.

II. ESPAR antenna

The 12-element ESPAR antenna used in the system described in this paper is shown in Fig. 1. The radiation pattern is controlled by changing the reactance applied to each passive element, or equivalently, the sequence of switching pre-set reactances connected to the passive elements. An example of the switching sequence with a sector duration of approximately 4 μs and hence rotation duration of about 48 μs is shown in Fig. 2.

The far-field radiation is produced by the summation of all the monopole patterns on the ground plane. The column vector $\boldsymbol{s}$, containing signals $s_m(t)$ (m= 0,1,...,M) impinging on antenna element m, is expressed as

$$\boldsymbol{s}(t) = \Sigma_{k=1}^{K} a(\phi_k) u_k(t), \quad (1)$$

where K is the number of signal directions, $u_k(t)$ is the transmitted signal with DoA ϕ_k and $a(\phi_k)$ is the architecture specific steering vector [3].

III. DoA algorithms

The application requires the ability to compute the angle in real-time together with a robustness to phase and noise. Two direction of arrival algorithms were investigated: namely cross-correlation and MUSIC.

A. Cross-correlation

The complex cross-correlation technique has the lowest implementation complexity with low-resolution but is robust

ISBN: 978-1-4799-6376-8/15/$31.00 ©2015 IEEE

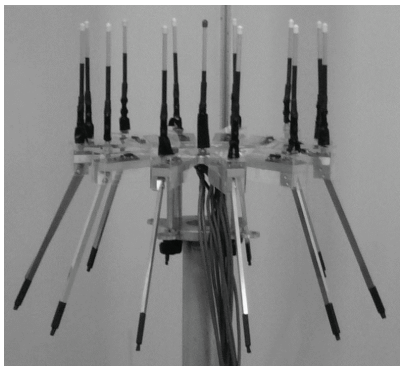

Fig. 1. Twelve-element ESPAR antenna used in the experiment consisting of 1 central RF port and 12 surrounding passive antennas.

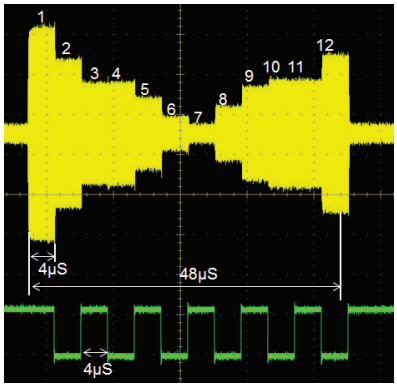

Fig. 2. Amplitude and duration of signal applied at each sector.

against phase fluctuations. It is calculated as (2) [4] [5]

$$P_{CC}(\theta) = \frac{\sum_{t=1}^{M} g(\theta,t)u^*(t)}{\sqrt{\sum_{t=1}^{M} g^2(\theta,t)}\sqrt{\sum_{t=1}^{M} u^2(t)}} \quad (2)$$

where θ is the integer angle index, M is the number of antenna elements, g is the reference antenna response and u is the received signal at time t. The cross-correlation of the reference antenna response at 0 deg. with that at angles {0,90,180,270} is shown in Fig. 3. The reference response was determined at one degree intervals in an anechoic chamber. The cross-correlation beamwidth is very broad and maximum dynamic range under ideal conditions is less than 10 dB.

B. MUSIC

The MUSIC algorithm, first proposed by Schmidt in [7], exploits the eigen-structure of the signal covariance matrix. The covariance is conventionally estimated from snapshots of signals arriving on each of the antenna array elements, and thus has to be modified for the ESPAR antenna which has a single RF port [8]. In the ESPAR-MUSIC algorithm, the antenna is virtually rotated by changing the load reactances on the elements at each sector period. The received down-sampled signal vector at time t is expressed as

$$\boldsymbol{U}(t) = [u_1(t), u_2(t), ..., u_M(t)] \quad (3)$$

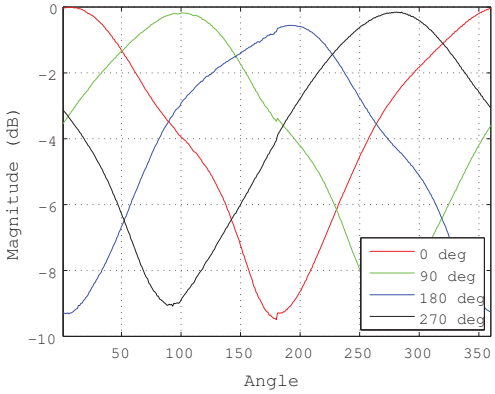

Fig. 3. Cross-correlation of the reference antenna response at 0 deg. with those at angles {0,90,180,270}.

The signal correlation matrix is then computed as

$$R_{UU} = E[\boldsymbol{u}(t)\boldsymbol{u}^H(t)] = (1/N_s)\boldsymbol{U}\boldsymbol{U}^H \quad (4)$$

where $\boldsymbol{u}$ represents the received signal vector averaged over the multiple revolutions as described in Section IV-C.

$\boldsymbol{R}_{UU}$ is eigen-decomposed and the eigenvalues are ranked low to high. The D most significant eigenvalues correspond to the impinging signals and the M-D smallest ones correspond to the noise eigenvalues, $\boldsymbol{E}_n$. The MUSIC spectrum is then obtained as

$$P_{MU}(\phi) = \frac{1}{|\boldsymbol{E}_n^H \alpha(\phi)|^2}, \quad (5)$$

where H is the Hermitian operator, $\alpha(\phi)$ is the steering vector measured in the anechoic chamber with angle resolution, res. MUSIC requires an exhaustive search through all steering vectors to estimate the DoA. That is, equation (5) is computed for all (360/res) discrete angles of ϕ.

In order to calculate (5), it is first necessary to estimate the number of noise subspaces. We use the Akaike Information Criterion (AIC) technique, which selects the most appropriate model that minimizes the distance between itself and actuality [9]. The number of directions corresponds to the model with the minimum AIC score.

IV. Experiment

A. Hardware

The receiver controller comprises a NI-PXIe-1071 PXI-Express chassis [10] containing NI-PXIe-5601 RF upconverter and NI-PXIe-5422 100 Ms/s cards (Fig. 4). At the TX, a sequence of PN random data bits are modulated using the $\pi/4$ D-QPSK scheme. At the RX, The ESPAR beam center sweeps through twelve directions at 30 degree intervals with an oversampling factor of twelve and hence there are 144 samples per antenna rotation. At each location, the main beam was rotated a total of 25,000 times. The system parameters are summarized in Table I.

ISBN: 978-1-4799-6376-8/15/$31.00 ©2015 IEEE

Fig. 4. Receiver equipment comprising NI-PXIe-1071 hardware controller and ESPAR antenna.

TABLE I. System Parameters.

Symbol rate	4800 Baud
Bandwidth	6.5 kHz
Tx Modulation	$\pi/4$ D-QPSK
Antenna sectors	12
Recorded oversampling factor	12
Combined samples per symbol	4
No. of rotations per location	25000
No. of rotations per MUSIC set	250
No. rotations between data in same MUSIC set	100

B. Field Measurement

The measurement carriage containing the ESPAR antenna and controller moved at about 20 km/h along an approximate 4 km stretch of a railway line in Kyoto prefecture, Japan. Starting at 100 m intervals, a data block of 25,000 ESPAR-rotations was recorded. An aerial photo showing the measurement locations is shown in Fig. 9. The locations marked in the map refer a distance marker. For example, the marker '32K1' indicates the position 32.1 km from the reference point. The locations of the Yagi-Uda directional transmit antennas are indicated by the yellow-blue asterisk at T1 and T2. Photos taken in direction of the yellow arrows at PA and PB are shown in Fig. 10 (a) and (b) respectively. In both photos the antenna T2 can be seen.

C. Post-processing

During post-processing, the four samples either side of the center were discarded and the center four samples were averaged. Strong in-band interference from very closeby transmitters was filtered in the frequency domain during the post-processing. As the symbol rate of 4800 Baud is relatively low, data is mostly modulated by the same symbol in successive rotations. The data was therefore multiplexed into 100 sets each comprising 250 rotations. The spacing between data used in each MUSIC calculation is 100 rotations and this ensures signals traversing several data symbols are present in each MUSIC DoA calculation (Fig. 5).

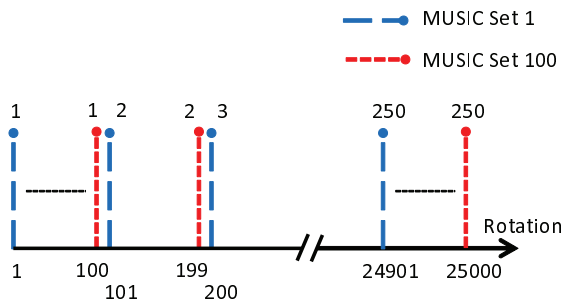

Fig. 5. Extraction of input data for post-processing with the MUSIC algorithm.

V. Performance Results

The MUSIC spectrum is calculated using Eq. (5) and the snapshot of the DoA with the highest angular dynamic range at the locations 32KX is shown in Fig. 8. A snapshot of the cross-correlation and MUSIC angular power spectrum at each map location is shown in Fig. 11. In general the estimated DoA pointed in the direction of the Tx base-station with the highest receive power. However in cross-over regions the receive power was almost equal and the predicted number of signal directions increased. Outside of the cross-over regions and also the regions affected by multipath, generally one DoA was found. A snapshot of the AIC score at locations 32KX shows that there are 11 noise eigenvalues and hence 1 principle signal direction is estimated (Fig. 6). The estimated number of directions are plotted in Fig. 7 along with the locations.

The estimated DoA at locations 32K5 and 32K4 point toward transmitter T1 (Fig. 11). These measurement positions are approximately 200 m and 100 m distance from the transmitter and a single, reasonably sharp, DoA is obtained. Although the beam-center at 32K3 does point East toward T1, the beam is considerably broadened, and it is conjectured that this is due to reflected signals off the West-side of the adjacent overpass. On the other side (East-side) of the overpass, the estimated DOA at 32K2 points toward T2 which is less than 20m away. The position 32K1 is on the other-side (right) of T2, and so we expect the following signal directions to flip approximately 180 deg. The beam at 32K1 does indeed point West, although its beamwidth is broadened, again most likely from multipath reflections off the West-side of the overpass. Measurements at 32K0 and 31K9 also point West. Although the DoAs at 31K8 and 31K7 do point towards T2 they are considerably broadened most likely due to reflections from the surrounding inclined land and buildings in their vicinity. The number of signal directions at these two positions as estimated using AIC is also greater than one. Residual in-band interference and also any differences between the in-situ antenna radiation pattern and that of the anechoic chamber reference will also account for some broadening.

VI. Conclusion

This paper has described a narrowband DoA estimation technique operating with mobility in the UHF band as part of a railway control system. Our experimental results show that the developed system can estimate the number of the component

ISBN: 978-1-4799-6376-8/15/$31.00 ©2015 IEEE

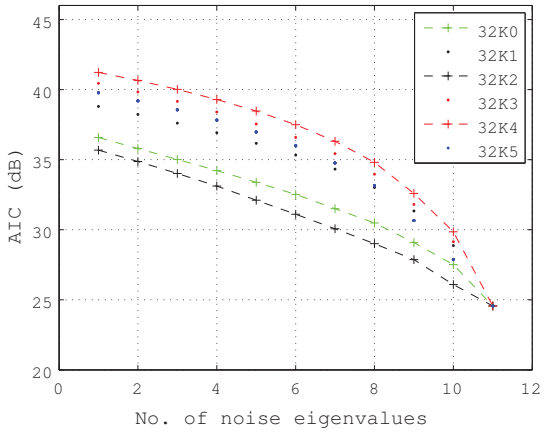

Fig. 6. AIC score versus number of noise eigenvalues at positions 32KX.

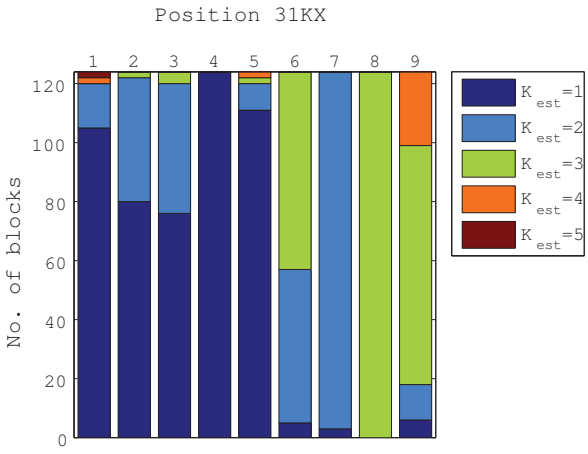

Fig. 7. Estimated number of signal directions using AIC at positions 31KX (X=1 to 9).

multi-path waves. At the measurement positions examined to date, the estimated DoA generally points in the direction of the nearest transmitter. The surrounding environment and antenna enclosure housing on the deck together with in-band interference also helps to explain the broadening of the estimated DoA. Further work will aim to improve the performance in the presence of interference.

ACKNOWLEDGEMENT

The authors gratefully acknowledge the support of West Japan Railway Company. This work was supported by JSPS KAKENHI Grant Number 24360144.

REFERENCES

[1] T. Ohira and K. Gyoda, "Electronically steerable passive array radiator antennas for low-cost analog adaptive beamforming," *Proc. IEEE Int. Conf. Phased Array Syst. Technol.*, Dana Point, California, May. 2000.

[2] European Commission, "High capacity network Architecture with Remote radio heads & Parasitic antenna arrays," *FP7 ICT Objective 1.1 Future Networks*, Feb. 2013.

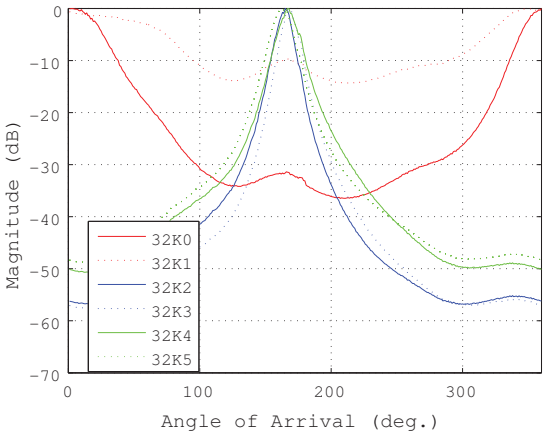

Fig. 8. MUSIC AoA snapshot with highest dynamic range at positions 32KX.

[3] C. Plapous J. Cheng, E. Taillefer, A. Hirata, and T. Ohira, "Reactance domain MUSIC algorithm for electronically steerable parasitic array radiator," *IEEE Trans. on Antennas and Propagat.*, vol. 52, No. 12, Dec. 2004.

[4] Y. Ozaki, J. Ozawa, E. Taillefer, J. Cheng, and Y. Watanabe, "A simple DoA estimator using adjacent pattern power ratio with switched beam antenna," *Progress in Electromagnetics Research*, vol. 22, 55-71, Oct. 2011.

[5] E. Taillefer, A. Hirata and T. Ohira, "Direction-of-arrival estimation using radiation power pattern with an ESPAR antenna," *IEEE Trans. on Antennas and Propagat.*, vol. 53, no. 2, Feb. 2005.

[6] W. Pannert, "Spatial smoothing for localized correlated sources - Its effect on different localized methods in the nearfield," *Elsevier Applied Acoustics*, Vol. 72, pp. 873–883, 2011.

[7] R. Schmidt, "Multiple emitter location and signal parameter estimation," *IEEE Trans. Antennas Propagat.*, vol. AP-34, No. 3, Mar. 1986, pp.276-280.

[8] C. Sun and C. Karmakar, "Direction of arrival estimation absed on a single port smart antenna using MUSIC algorithm with periodic signls," *World Academy of Science, Eng. & Tech.*, pp. 984–993, 2007.

[9] M. Wax and T. Kailath, "Detection of signals by information theoretic criteria," *IEEE Trans. on Acoustics, Speech and Signal Processing*, vol. ASSP-33, 387-392, Feb. 1985.

[10] National Instruments, "NI-PXIe-1071 4-slot 3U PXI Express Chassis," *Datasheet*, 2012.

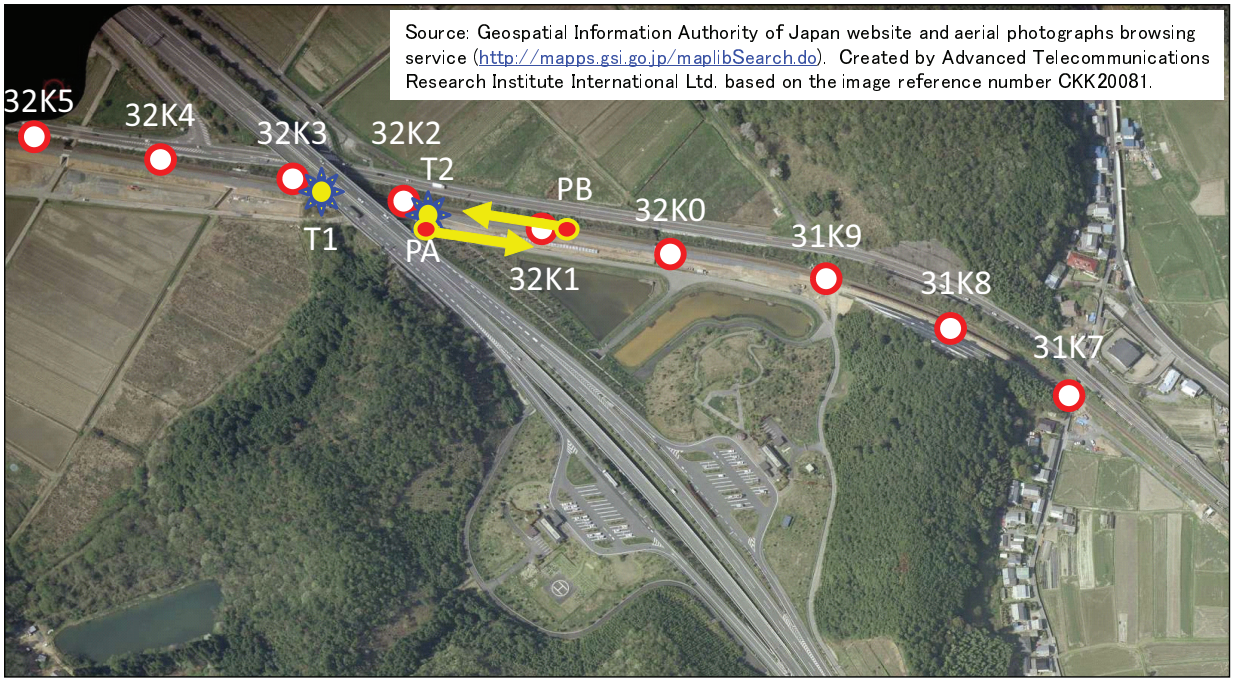

Fig. 9. Map showing Tx locations {T1,T2}, photo vantage points {P1,P2} and Rx locations 31K7 to 32K5.

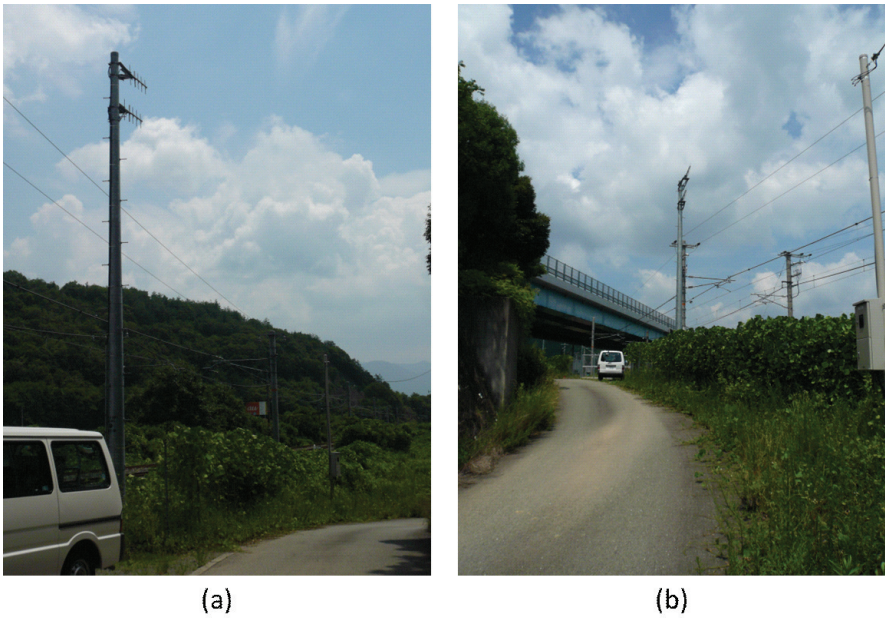

Fig. 10. Photo looking in direction of arrows with Yagi-Uda transmit antenna T2 visible at (a) position PA, (b) position PB.

ISBN: 978-1-4799-6376-8/15/$31.00 ©2015 IEEE

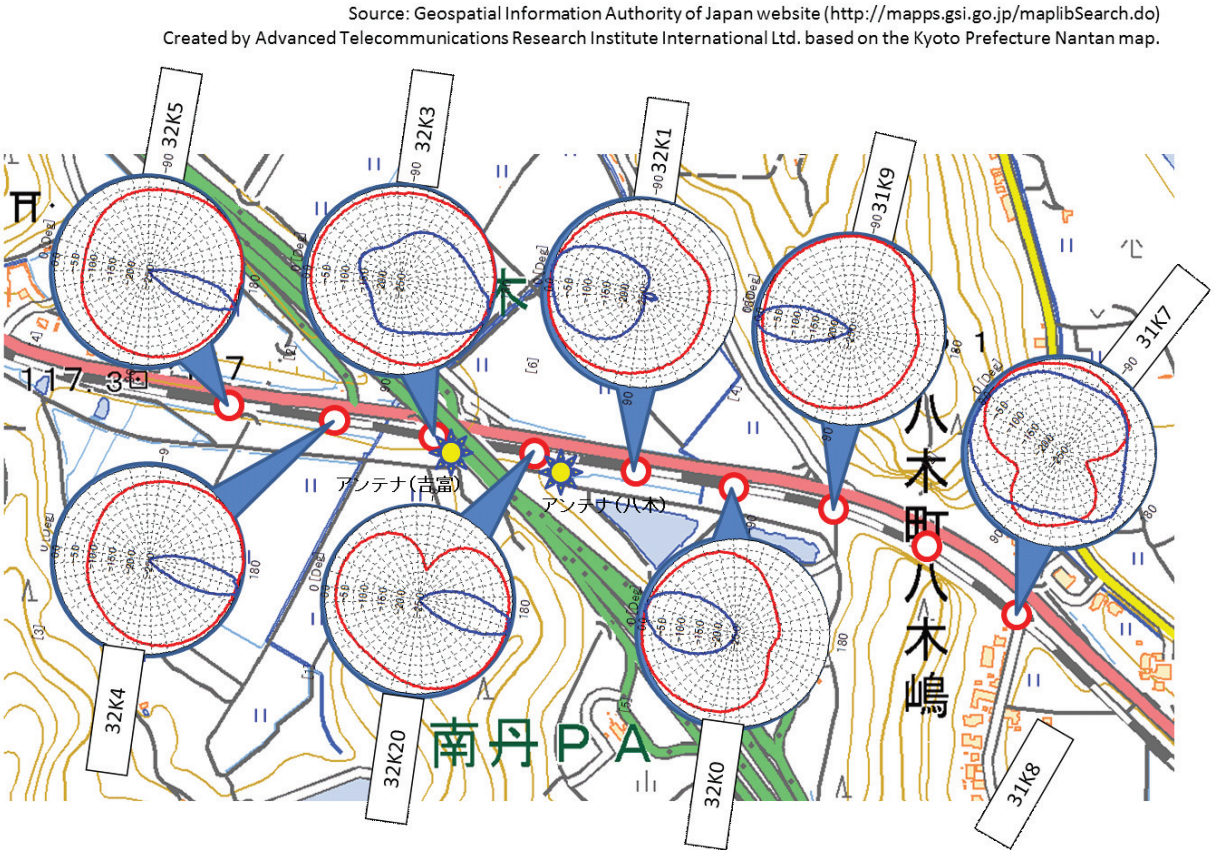

Fig. 11. AoA snapshot at locations 31K7 to 32K5.

ISBN: 978-1-4799-6376-8/15/$31.00 ©2015 IEEE